*Egypt. J. Chem.* **Vol. 66**, No. 7 pp. 439 - 449 (2023)

**Egyptian Journal of Chemistry**

**http://ejchem.journals.ekb.eg/**

# Iron-Trimesic Metal Organic Frameworks as Nano-Adsorbents for Tetracycline and Ceftriaxone Contaminated Wastewater Effluents

**Hossam F. Nassar,[a] Alzahraa Shaban,[b] Amal Zaher,[c] Taha Abdelmonein,[b] Esaraa Salama,[d] Yasser Gaber,[e] Nabila Shehata,[f] Reda Abdelhameed,[g] Rehab Mahmoud[b]***

[a] *Department of Environmental Sciences and Industrial Development, Faculty of Post Graduate Studies for Advanced Sciences, Beni-Suef university*

[b] *Chemistry Department. Faculty of Sciences. Beni-Suef University. Beni-Suef Egypt.*

[c] *Environmental Sciences and Industrial Development Department. Faculty of Postgraduate Studies for Advanced Sciences. Beni-Suef University. Beni-Suef Egypt. Egypt beni-Suef University.*

[d] *Biotechnology Department. Faculty of Postgraduate Studies for Advanced Sciences. Beni-Suef University. Beni-Suef Egypt.*

[e] *Department of Materials Science and Nanotechnology, Faculty of Postgraduate Studies for Advanced Sciences, Beni-Suef University, Beni-Suef 62511, Egypt.*

[f] *ESID dep., PSAS Faculty, Beni-Suef University, 62511 Beni-Suef, Egypt.*

[g] *Applied Organic Chemistry Department, National Research Centre, 33 EL Bohouth st., Dokki, Giza, Egypt.*

**Abstract**

Antibiotics release has been identified as a series concern with adverse effects on the ecosystem. Nano-adsorbents are promising materials to remove antibiotics from wastewater effluents. In this work, iron-trimesic metal organic frameworks (Fe-BTC MOF) was synthesized and characterized by XRD, FTIR, SEM and TEM. Fe-BTC was then investigated as nano-adsorbent for tetracycline (TC) and Ceftriaxone sodium (CFTR) antibiotics. TC and CFTR are common antibiotics, which are extensively used by industrial activities and thereby are released to wastewater effluents. Fe-BTC MOF showed high adsorption capacity of 713 and 1284.6 mg/g for TC and CFTR respectively. This study aims to compares the uptake efficiencies for two drug residues. Single antibiotic residues adsorption tests showed that Fe-BTC MOF effectively takes up TC more than CFTR. The influence of pH, dose, concentration and time on the adsorption process was estimated. Such adsorption capacity of Fe-BTC will make it favorable for further environmental applications.

*Keywords:* Fe-BTC MOF; Wastewater; Adsorption; Tetracycline; Ceftriaxone sodium

## 1. Introduction

The presence of antibiotics in soil and water streams has been a critical and urgent environmental challenge all around the world [1]. Sources of antibiotics discharged to the environment include agricultural run offs, wastewater treatment plants and pharmaceutical manufacturers wastewater effluents [2]. These antibiotics are extensively used in pharmaceuticals and personal care products (PPCPs) in various industrial activities and products such as livestock farming, skincare products, and cosmetics to name a few [3]. The improper discharge of such products and the lack of full treatment of industrial waste effluent streams are the main causes for the antibiotics leakage to the ecosystem. It is of urgent need to design, test, optimize and operate efficient processes and technologies that can treat wastewater streams and remove such leaked antibiotics at high efficiencies and low costs [4]. Several technologies already exist and are still under continuous improvement such as advanced electrochemical oxidation, membrane filtration, photocatalytic degradation and adsorption [5–9]. The latter is one of the most studied technologies due to its simple nature and low cost. Numerous types of adsorbents have been already utilized for antibiotics adsorption

*Corresponding author e-mail: prof.rehab.mahmoud@gmail.com.; (Prof. Rehab Khaled).

EJCHEM use only: Received date 31 July 2022; revised date 23 September 2022; accepted date 09 November 2022

DOI: 10.21608/EJCHEM.2022.153568.6647

including activated carbons and polymeric based adsorbents [10]. On the other hand, there still exists a persistent need to develop enhanced adsorbents, which are more efficient, more stable, have high removal capacity and shows fast adsorption kinetics [10,11].

Among several promising candidates as antibiotic adsorbents, metal-organic frameworks (MOFs) emerged as one of the best [12]. MOFs has high water stability, high surface area, adjustable functionalities and tailored morphology [12,13]. In particular, iron based MOFs (Fe-MOFs) has been recognized as a promising category of MOFs due to the abundance and non-toxicity of iron as an element [3,14–16].

Among the most common types of Fe-MOFs are Fe-BTC, MIL-100-Fe and MIL101-Fe which have been the centre of focus recently as adsorbents for wastewater treatment [17]. Fe-BTC (BTC: 1,3,5-benzenetricarboxylate) is typically formed as a semi-amorphous network of locally ordered subunits of Ferric ions and acetate moieties [18,19]. Fe-BTC is considered as a very promising candidate for practical water treatment applications due to its low cost and its ease of synthesis and is expected to have high adsorption capacities for several pollutants [20]. That is why, in this study, Fe-BTC was chosen as a model Fe-MOFs for antibiotic adsorption from simulated wastewater streams.

In this work, two of the most common antibiotics were selected as models to investigate the adsorption capacity and kinetics of Fe-BTC MOF namely, tetracycline (TC) and Ceftriaxone sodium (CFTR). TC is one of the most common wide spectrum tetracycline type antibiotics used as an additive (for animal growth promotion) and for treating bacterial infections [21]. Moreover, TC is a typical additive in PPCPs and have numerous properties that hinder its treatment using conventional processes such as its highly stable aromatic structure, high polarity, water solubility and toxicity [3]. The presence of tetracyclines generally in water, soil, sediments and animal wastes requires extensive studies to investigate its removal to mitigate their adverse effects on the ecosystem [22]. In this study, TC was chosen as a model pollutant and as a representative for the tetracyclines antibiotics.

On the other hand, CFTR is a third generation cephalosporin antibiotic, which is widely used due to its low toxicity and allergic reactions [23]. CFTR can act on both Gram-positive and Gram-negative bacteria [24]. CFTR has been identified as one of the common antibiotics discharged in rivers which in consequence have adverse effects of photosynthesis of plants and human health. Both TC and CFTR were chosen in this study as model pollutants to be removed by Fe-BTC.

Recently, Zhou et al reported the use of a simple precipitation technique (as reported by [25]) to prepare Fe-BTC and tested it for the single and competitve adsorption of TC and norfloxacin from wastewater [26]. The authors reported a maximum TC adsorption capacity of 714.3 mg/g and 682.5 mg/g for the single and binary systems respectively. Fe-BTC showed high adsorption capacity, high selectivity and excellent recyclability [26]. Zhao et al tested several MOFs (including Fe-BTC) as single standing adsorbents or impeded into chitosan matrix for TC adsorption [10]. The Fe-BTC chitosan composite showed an adsorption capacity of 65 mg/g and 85% removal effeciciency for TC.

On the other hand, no previous study has reported the use of MOFs as adsorbents for CFTR. Therefore, the aim of the current work was to synthesize and characterize Fe-BTC MOF using various characterization techniques. The prepared Fe-BTC MOF was then used as a nano-adsorbent for TC and CFTR. The effect of pH, adsorption dose, initial concentration and adsorption kinetics were studied. Finally, a comparison between the performance of Fe-BTC MOF for TC and CFTR adsorption was conducted with other similar material reported in the open literature. This study paves the road towards developing Fe-BTC based MOFs with high adsorption capacities and multi-functional properties for the removal of challenging wastewater contaminants.

## 2. **Experimental**

### *2.1. Materials and methods*

Iron nitrate.$9H_2O$ (SDFCL company, India) and N,N-dimethyl formamide (DMF, 99.9%) were purchased from Sigma–Aldrich Co. Benzene-1,3,5-tricarboxylic acid (H3BTC, 98%) was obtained from Merck, (Darmstadt, Germany). Tetracycline HCL was gotten from Hebe (China). All the chemicals used are high-purity grade chemicals, and the solvents used were of spectroscopic grade. NaOH and hydrochloric acid were purchased from Piochem for laboratory chemicals (Egypt) and Carlo Erba,

(France) respectively.

### *2.2. Synthesis of Fe-BTC MOF*

Fe-BTC was prepared by solvothermal method as described in our previous work [27]. Briefly 1.0 g of H3BTC was dissolved in 30 mL of DMF; the resulted solution was mixed with a solution made of 2.0 g of $Fe(NO_3)2{\cdot}9H_2O$ and 20 mL of DMF. The mixture was sonicated for 15 min and then heated in an oven at 110 ºC for 6 h. The resultant material was filtered and washed several times then dried overnight.

### *2.3. Characterization of the prepared samples*

The prepared adsorbent was characterized by using different tools; Panalytical (Empyrean) X-ray diffractometer with Cu-Kα radiation operated at a current of 35 mA and voltage 40 kV, is used to determine the crystallinity and the structural composition of the synthesized material as discussed in our previous work [28]. IR spectra were recorded on a (Bruker-Vertex 70, Germany) Spectrometer at the wave number range of 4000-400 cm-1. Moreover, the microstructure and the morphology of the synthesized materials were investigated using Field Emission Scanning Electron Microscope (FESEM). The BET analysis for specific surface area, pore size distribution and specific pore volume of the prepared samples were determined (TriStar II 3020, Micrometrics, USA).

### *2.4. Adsorption study*

Adsorption experiments were conducted in batch method to determine the effect of solution pH, adsorbent dose, contact time, and initial concentration of TC. The study on the effect of pH was carried out at pH = 3-10, the pH of solutions was adjusted by 0.1 M HCl and NaOH solutions and the effect of adsorbent dosage was investigated using various masses of adsorbent (0.015g to 0.20g). Stock solution of TC was prepared by dissolving TC into distilled water (DW). During the adsorption study, the syringe filter (membrane 0.45μ) was used for solid-liquid separation via a filter and the TC in the filtrate were detected by using UV–visible spectrophotometer (UV-2600, Shimadz, Japan). The maximum wavelength of TC was observed at 276 nm [29]. For the isotherm adsorption study, the flasks containing reaction solutions (adsorbent dose = 0.05g of adsorbent into 20 mL TC solution, pH = 5.0, initial concentration = 5 ~ 1000 mg/L) were sealed and placed in shaker at the room temperature, shaken for 24h at the speed of 300 rpm, the isotherm models described below.

Models used to describe adsorption isotherms are summarized below [5,30–33]:

| | | |
|---|---|---|
| *Langmuir:* | $q_e = (K_L q_m C_e)/(1+K_L C_e)$ | *(1)* |
| *Freundlich:* | $q_e = K_F C_e^{1/n}$ | *(2)* |
| *Langmuir-Freundlich:* | $q_e = KC_e^{1/n} /1+bC_e^{1/n}$ | *(3)* |
| *Dubinin-Radushkevich:* | $lnq_e = K_{DR}R^2T^2ln^2 ( +1/C_e) + lnq_{DR}$ | *(4)* |
| *Redlich-Peterson:* | $q_e = Ac_e/1 + BC_e^{\beta}$ | *(5)* |
| *Khan:* | $q_e = (q_m b_k C_e)/(1+ b_k C_e)^{ak}$ | *(6)* |
| *Toth:* | $q_e = (K_e C_e)/(1+K_L C_e)^{1/n}$ | *(7)* |
| *Sips* | $q_{e=} q_m K_s C_e^{1/n}/1 + K_s C_e^{1/n}$ | *(8)* |
| *Baudu:* | $q_e = \frac{q_m bo\, C_e^{1+x+y}}{1 + boC_e^{1+x}}$ | *(9)* |
| *Fritz-Schlunder:* | $q_e = \frac{q_{mFss}\, K1\, C_e^{m1}}{1 + K2\, C_e^{m2}}$ | *(10)* |

Specially, for the adsorption kinetics study, adsorbents were added into conical flasks with stopper, separately at given time (5 ~ 90 min), then taken out and filtered immediately to collect the filtrate. The filtrate was then detected by UV–visible spectrophotometer, the used kinetic models were pseudo-first-order, pseudo-second order, Intraparticle diffusion model, mixed 1, 2-order and Avrami model as shown below.

| | | |
|---|---|---|
| *pseudo-first order* | $q_t = q_e (1 - exp (- K_1 * t)$ | *(11)* |
| *pseudo-second order* | $q_t = (K_2 * t * q_e \text{ ^2}) / ( 1 + K_2 * t * q_e )$ | *(12)* |
| *intra-particle diffusion* | $q_t = K_{ip} (t \text{ ^ } 0.5) + C_{ip}$ | *(13)* |
| *mixed model* | $q_t = q_e ((1 - exp (- K * t) / (1- f_2 * (1 - exp (- K * t))$ | *(14)* |

where $q_e$ and $q_t$ are the antibiotics quantities adsorbed at equilibrium and at various time intervals, respectively. $K_1$ and $K_2$ are the adsorption rate constants [34]. Moreover, $f_2$ is the dimensionless coefficient of mixed first and second order and k is the adsorption rate constant [35].

## 3. Results and discussion

### *3.1. MOF sample characterization*

Figure 1a shows the xrd diffraction pattern of Fe-BTC MOF sample. The xrd pattern shows no distinctive peaks reflecting the amorphous nature of the prepared MOF. This is a typical behaviour for Fe-BTC MOF as previously reported by several studies [36,37]. Figure 1b illustrates the FTIR transmittance spectrum of the Fe-BTC MOF powder. The broad peak at 3421 $cm^{-1}$ is attributed to the OH stretching due to the adsorbed water molecules [38,39]. The peak at 1717 $cm^{-1}$ can be attributed to the C=O group in Fe-BTC structure. Moreover, the peaks at 1630 cm-1 and 1560 $cm^{-1}$ are assigned to the C=C bond in the aromatic ring [40]. The peaks at 1456 $cm^{-1}$ and 1375 cm-1 can be attributed to the asymmetric and symmetric stretching vibrations of the O-C-O groups respectively [38]. The peak at 1114 cm-1 is attributed to the C-O-Fe bond in the MOF structure [40]. The peaks at 946 $cm^{-1}$, 785 $cm^{-1}$ and 711 $cm^{-1}$ are attributed to the C-$CO_2$ bond described in previous reports [41,42]. Finally, the peak at 630 cm-1 is due to the stretching vibration of Fe-O bond [43].

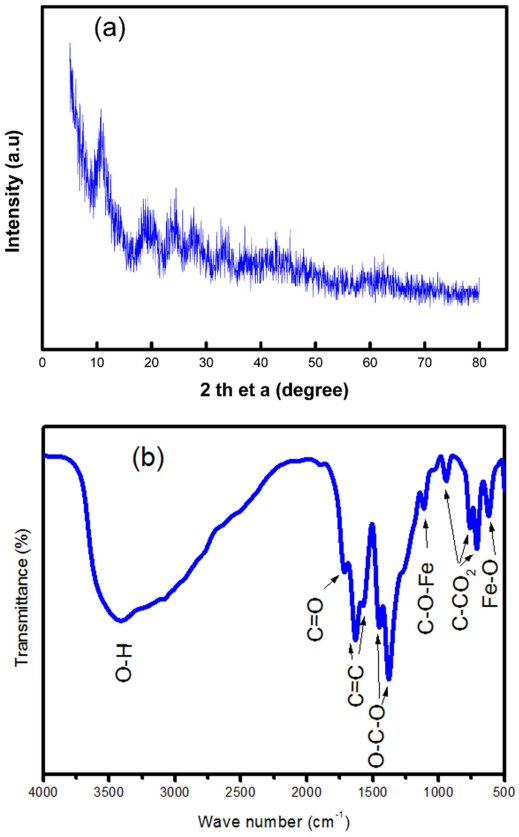


**Fig. 1:** (a) XRD and (b) FTIR of the Fe-BTC MOF sample before adsorption

Figure 2 shows the scanning and transmission electron microscope images along with the Edx spectrum of the Fe-BTC MOF sample. As shown in figure 2a, the sample consists of irregular sphere like aggregated particles. Upon further magnification, it is observed that the aggregates are composed of fine smaller spherical particles as shown in figure 2b. The TEM image (figure 2c) confirms the small particle size of the MOF nanoparticles being the range 30-50 nm. The Edx spectrum of the prepared Fe-BTC MOF was measured as shown in figure 2d. This spectrum illustrates peaks for Fe, C and O without any extra peaks. The lack of any impurity signals reflects the purity of the prepared Fe-BTC MOF sample.

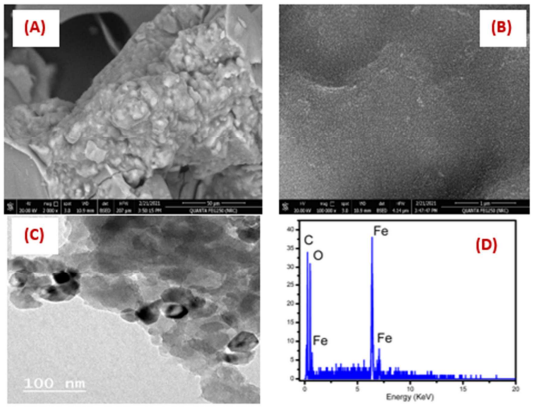


**Fig.** 2: (a) And (b) SEM images, (c) TEM and (d) Edx spectrum of the Fe-BTC MOF sample before *adsorption.*

### *3.2. Tetracycline adsorption study*

#### *3.2.1. Effect of pH*

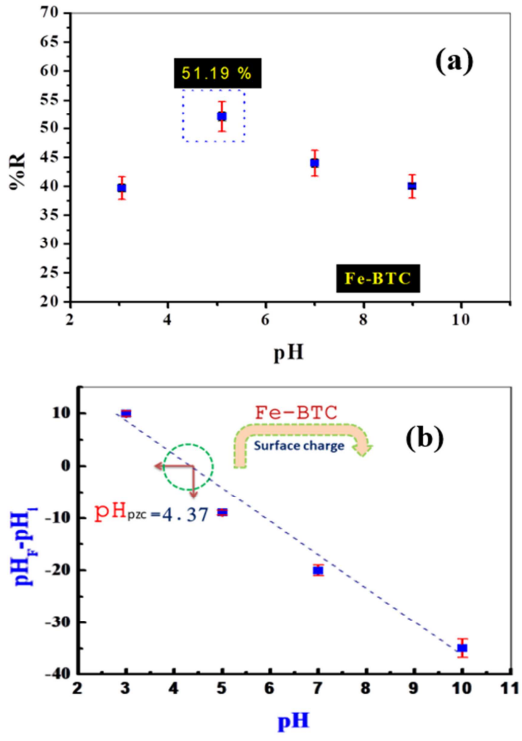


**Fig. 3:** *(a) Effect of pH on adsorption of TC onto Fe-BTC MOF ($V_{TC}$ 30 ml, adsorbent mass 0.01 g: agitation speed = 380 rpm, T = 25±0.5 °C and Co = 100 ppm)(a) and the surface of adsorbent charge- pH curve (b).*

The pH has a major effect for uptake the pollutant species from wastewater [44]. The pH effect on the ionization process of TC molecule, which may be generate different active binding sites. The TC solution pH also effects on the charge of the adsorbent. Fig.3(a) displays the influence of pH (from 2.0 to 10) on TC uptake onto the Fe-BTC samples (at $C_o$ 100 ppm TC solution). The collected results prove that the TC solution pH has a high effect on the efficiency of adsorpent for TC uptake. When the pH of the solution was less than $pKa_1$ (3.57) [45], the TC uptake was found to be 38 %. In the acidic conditions, the TC species present as cationic shape; and the surface of the adsorpent have positive charges (PZC= 4.37) [45]. Thus, the lowering in the TC uptake at low pH is may be due to the electrostatic repulsion. The TC removal was sharply increased and was found to be 51.19 % at the value of pH 5.

#### *3.2.2. Effect of amount of adsorbent*

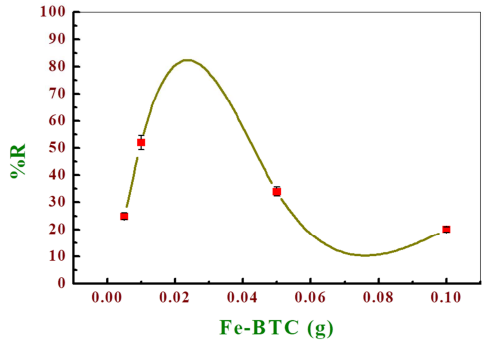


**Fig. 4:** *Effect of amount of Fe-BTC on adsorption of TC proces ($V_{TC}$ 30 ml, pH 5, agitation speed = 380 rpm, T = 25±0.5 °C and Co = 100 ppm)*

Figure 4 illustrated the influence of the Fe-BTC dose (0.005–0.15 g) on TC removal with 100 ppm as an initial concentration at pH ~ 5. It was observed that the percentage of the adsorption efficiency had increased with the increasing dosage of the adsorbent. The presence of many active sites was found to be higher as the amount of the adsorbents increases. As shown in Fig. 4 using little amounts of the adsorbent is better compared to higher doses, as it results in decreasing the process overall cost. Additionally, using small amounts of nanoparticles is faviurable in the industrial applications, while increasing the weight will produce a negative overall economic and technical impact. The best dose was at 0.03 g.

### 3.2.3. Effect of initial concentration

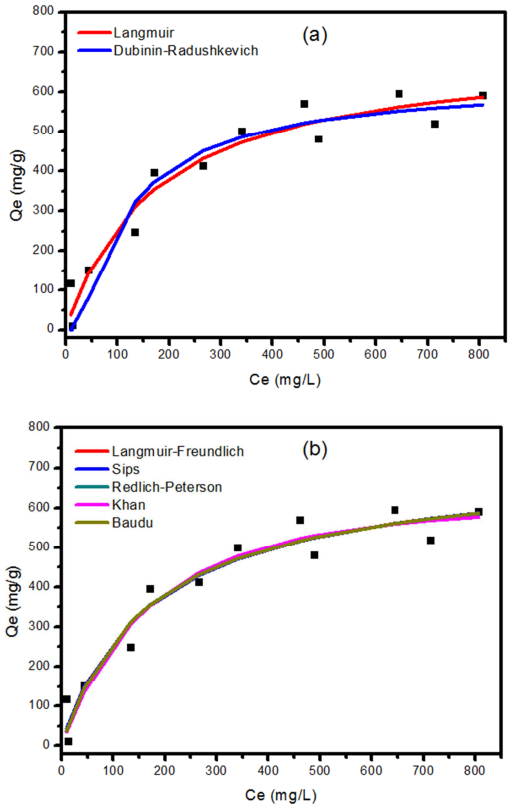


**Fig. 5:** *Isotherm models fitting for the TC adsorption isotherm.*

The equilibrium of adsorption is one of the important physico-chemical aspects in the description of adsorption behavior. In this work, seven well-known models of Langmuir, Freundlich, Langmuir-Freundlich, Dubinin–Radushkevich Redlich-Peterson, Sips, Khan and Baudu isotherm are evaluated. The best fitting of isotherm equations is compared by judging the highest correlation coefficients $R^2$. To follow, the parameters of the models are calculated and iluustrated (Table 1). The best fit was shown to be that of Langmuir adsorption model representing a mono-layer adsorption with $R^2$ = 0.95. No further improvement in the value of $R^2$ was calculated for higher parameter isotherm models.

**Table 1**

Adsorption isotherm fitting parameters for CFTR adsorption onto Fe-BTC MOF

| Adsorption models | Parameter | |
|---|---|---|
| Langmuir | $q_{max}$ (mg/g) | 713 |
| | $K_L$ (L/mg) | 0.0057 |
| | $R^2$ | 0.95 |
| Langmuir-Freundlich | $q_{max}$(mg/g) | 731.14 |
| | $K_{LF}$ (L/mg) | 0.0054 |
| | $M_{LF}$ | 0.94 |
| | R2 | 0.94 |
| Dubinin–Radushkevich | $q_{DR}$ (mg/g) | 635.14 |
| | $K_{DR}$ | 0.0183 |
| | $R^2$ | 0.92 |
| Redlich-Peterson | $K_R$ | 3.95 |
| | $a_R$ | 0.0045 |
| | β | 1.03 |
| | $R^2$ | 0.95 |
| Khan | $q_m$ (mg/g) | 995.95 |
| | $b_K$ | 0.0037 |
| | $a_K$ | 1.18 |
| | $R^2$ | 0.94 |
| Sips | $Q_m$ | 730.76 |
| | $K_s$ | 0.007 |
| | 1/n | 0.95 |
| | $R^2$ | 0.94 |
| Baudu | $q_m$ (mg/g) | 546.19 |
| | $b_0$ | 0.0069 |
| | x | 0.035 |
| | y | 0 |
| | $R^2$ | 0.94 |
| Fritz-Schlunder | $q_{mFSS}$ | 177.52 |
| | $K_1$ | 0.27 |
| | $K_2$ | 0.28 |
| | $m_1$ | 0.41 |
| | $m_2$ | 0.000048 |
| | $R^2$ | 0.91 |

### 3.2.4. Kinetics investigation

Kinetics of TC adsorption is shown in figure 6 and the estimated parameters are summarized in table 2. From the experimental data, it is obvious clear that the uptake efficiency of TC onto the Fe-BTC increases rapidly during the early time of adsorption due to the existence of the vacant active centers, till the time interval of 10 min (Fig. 6 ). After 10 min, the equilibrium state was reached. The adsorption process was best fitted with the Pseudo First Order

and the Avrami model, with $R^2$ value of 0.95.

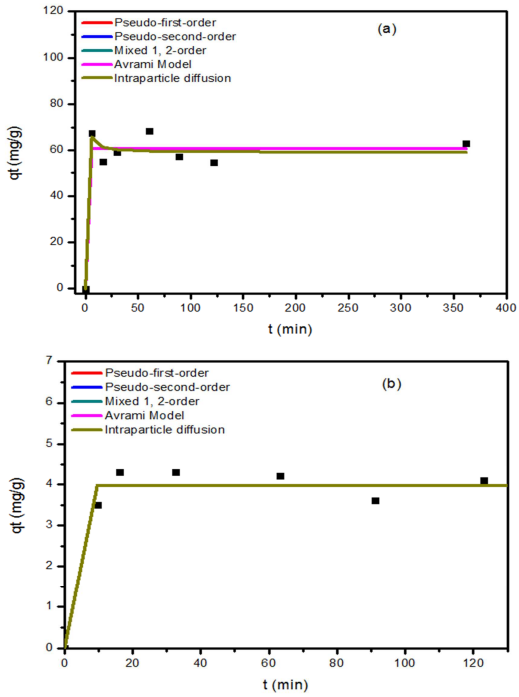


**Fig. 6:** *Fitting of adsorption kinetic models (Pseudo first order, pseudo second order, mixed and intraparticle diffusion) of TC at initial concentration (a) 20 mg/L and (b) 50 mg/L onto Fe-BTC.*

**Table 2**

The parameters of kinetic models for the TC adsorption onto Fe-BTC

| Model | Parameters | Values (20 mg/L) | Values (50 mg/L) |
|---|---|---|---|
| Pseudo First Order | $K_1$ ($min^{-1}$) | 4.04 | 4.045 |
| | $q_e$ (mg/g) | 60.81 | 3.97 |
| | $R^2$ | 0.94 | 0.95 |
| Pseudo Second Order | $K_2$ (g/(mg min)) | 187.46 | 187.46 |
| | $q_e$ (mg/g) | 60.81 | 3.97 |
| | $R^2$ | 0.94 | 0.71 |
| Intraparticle diffusion | $K_{ip}$ | 1.777 | 0 |
| | $C_{ip}$ | 40.05 | 3.97 |
| | $R^2$ | 0.22 | 0.71 |
| Mixed first and second order | K (g/(mg min)) | 0.00025 | 1 |
| | $q_e$ (mg/g) | 59.2 | 3.97 |
| | f2 | 1 | 3 |
| | $R^2$ | 0.95 | 0.71 |
| Avrami model | $K_{av}$ ($min^{-1}$) | 1.84 | 1.84 |
| | $n_{av}$ | 1.74 | 1.74 |
| | $q_e$ (mg/g) | 60.81 | 3.97 |
| | $R^2$ | 0.94 | 0.95 |

### *3.3. Ceftriaxone adsorption study*

Table 3 summarizes the estimates values of fitting parameters and the corresponding $R^2$ values for each model. The results demonstrated that the Langmuir model is the most adequate two parameter model in case of using Fe-BTC MOF for CFTR adsorption because it showed the highest adsorption capacity with the best fit ($R^2$ 0.93). However, three parameter models resulted in higher values of $R^2$ reaching 0.98 for the Langmuir-Freundlich model. No further improvement was observed for higher parameter models.

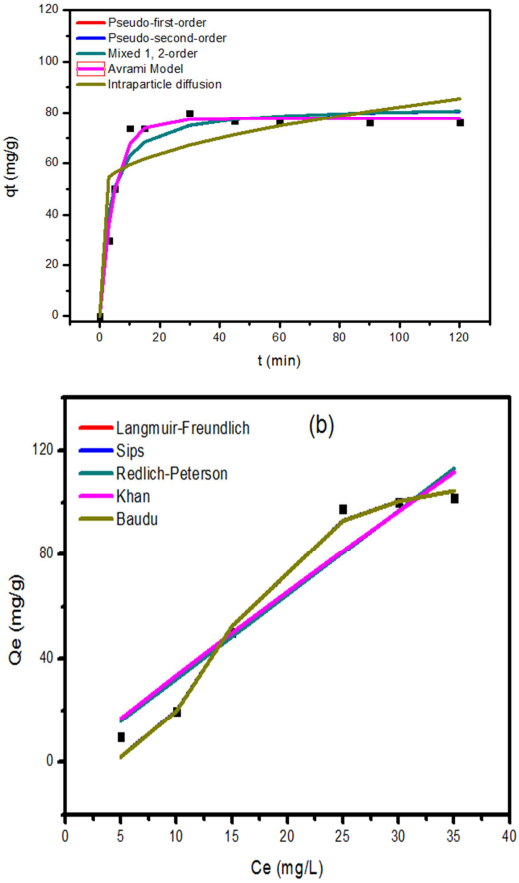


**Fig. 7:** *(a) Two and (b) Three parameter fitting for the CFTR adsorption isotherm.*

**Table 3**

Adsorption isotherm fitting parameters for CFTR adsorption onto Fe-BTC MOF

| Adsorption models | Parameter | |
|---|---|---|
| Langmuir | $q_{max}$ (mg/g) | 250.0 |
| | $K_L$ (L/mg) | 0.0027 |
| | $R^2$ | 0.93 |
| Langmuir-Freundlich | $q_{max}$(mg/g) | 110.62 |
| | $K_{LF}$ (L/mg) | 0.064 |
| | $M_{LF}$ | 3.475 |
| | $R^2$ | 0.98 |
| Dubinin–Radushkevich | $q_{DR}$ (mg/g) | 196.87 |
| | $K_{DR}$ | 0.0041 |
| | $R^2$ | 0.97 |
| Redlich-Peterson | $K_R$ | 3.24 |
| | $a_R$ | 0.004 |
| | β | 0 |
| | $R^2$ | 0.93 |
| Khan | $q_m$ (mg/g) | 595.47 |
| | $b_K$ | 0.00576 |
| | $a_K$ | 0.39 |
| | $R^2$ | 0.93 |
| Sips | $Q_m$ | 110.63 |
| | $K_s$ | 7.3E-05 |
| | 1/n | 3.47 |
| | $R^2$ | 0.98 |
| Baudu | $q_m$ (mg/g) | 106.32 |
| | $b_0$ | 7.05E-05 |
| | x | 0.01 |
| | y | 2.49 |
| | $R^2$ | 0.98 |
| Fritz-Schlunder | $q_{mFSS}$ | 77.04 |
| | $K_1$ | 0.11 |
| | $K_2$ | 2.12 |
| | $m_1$ | 1.02 |
| | $m_2$ | 4.82E-05 |
| | $R^2$ | 0.93 |

**Table 4**

The parameters of kinetic models for the CFTR adsorption onto Fe-BTC MOF

| Model | Parameters | Values |
|---|---|---|
| Pseudo First Order | $K_1$ ($min^{-1}$) | 0.2 |
| | $q_e$ (mg/g) | 77.5 |
| | $R^2$ | 0.96 |
| Pseudo Second Order | $K_2$ (g/(mg min)) | 0.0038 |
| | $q_e$ (mg/g) | 82.77 |
| | $R^2$ | 0.87 |
| Intraparticle diffusion | $K_{ip}$ | 3.34 |
| | $C_{ip}$ | 48.88 |
| | $R^2$ | 0.51 |
| Mixed first and second order | K (g/(mg min)) | 0.00024 |
| | $q_e$ (mg/g) | 82.76 |
| | $f_2$ | 0.99 |
| | $R^2$ | 0.87 |
| Avrami model | $K_{av}$ ($min^{-1}$) | 0.46 |
| | $n_{av}$ | 0.43 |
| | $q_e$ (mg/g) | 77.50 |
| | $R^2$ | 0.98 |

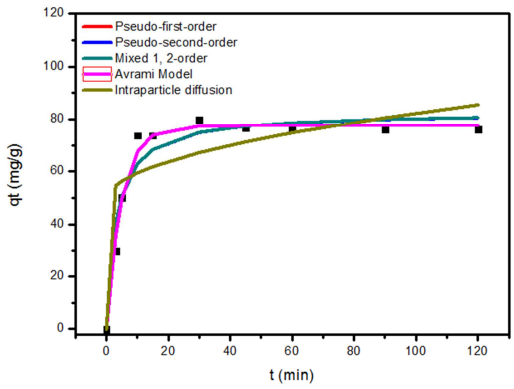


**Fig. 8:** *Kinetics models fitting for CFTR adsorption on Fe-BTC MOF*

Kinetics of CFTR adsorption is shown in figure 8 and the estimated parameters are summarized in table 4. The adsorption process was best fitted with the Avrami model, with $R^2$ value of 0.98.

Table 5 shows the comparison of adsorption results with similar studies in the open literature. Fe-BTC MOF shows very high adsorption capacity for both antibiotics as illustrated by the adsorption capacity of 713 and 1284.6 mg/g for TC and CFTR respectively.

**Table 5**

Recent studies reporting the adsorption of TC and CFTR compared to the current study

| Adsorbent | Removal capacity for TC (mg/g) | Reference | Adsorbent | Removal capacity for CFTP (mg/g) | Reference |
|---|---|---|---|---|---|
| Fe-BTC MOF | 713 | (This work) | Fe-BTC MOF | 1284.6 | (This work) |
| biochar | 26 | [46] | Bentonite-titanium oxide-chitosan | 90.9 | [47] |
| ZIF-8 metal organic-framework | 122.0 | [21] | Pseudomonas putida biomass | 109.5 | [48] |
| Zr/Fe-MOFs/GO composites | 158 | [49] | ferrihydrite/silica rice husk | 139 | [50] |
| Fe-BTC | 714.3 | [26] | organo-zeolite | 0.7288 | [51] |

## 4. Conclusions

In this work, iron-trimesic metal organic frameworks (Fe-BTC MOF) were successfully synthesized using a simple solvothermal method. The prepared sample was characterized by XRD, FTIR, SEM and TEM. Moreover, the synthesized sample was investigated for tetracycline (TC) and Ceftriaxone sodium (CFTR) antibiotics removal from wastewater effluents by adsorption. Fe-BTC MOF showed high adsorption capacity of 713 and 1284.6 mg/g for TC and CFTR respectively. Results show the promising nature of Fe-BTC MOF for the adsorption of antibiotics from wastewater streams. This study open the way for the preparation and investigation of various Fe-BTC MOF nanocomposites as nano-adsorbents for wastewater removal. Such composites are expected to show promising removal capacities and multi-functionality towards wastewater pollutants such as heavy metals, dyes, antibiotics and pathogens.

## 5. Conflicts of interest

"There are no conflicts to declare".

## 6. Formatting of funding sources

The authors of this work gratefully acknowledge the generous financial support from Beni-Suef University, University performance development centre, support and project finance office, project ID # BSU-CP7-19014.

## 7. References

[1] M. Gavrilescu, Water, soil, and plants interactions in a threatened environment, Water. 13 (2021) 2746.

[2] M. Hassouna, R.R. Amin, A.A. Ahmed-Anwar, R.K. Mahmoud, Efficient Removal of Oxytetracycline and Some Heavy Metals from Aqueous Solutions by Mg-Al Layered Double Hydroxide Nanomaterial, Egypt. J. Chem. (2019) 0–0. doi:10.21608/ejchem.2019.6102.1510.

[3] Z. Zhang, Y. Chen, Z. Wang, C. Hu, D. Ma, W. Chen, T. Ao, Effective and structure-controlled adsorption of tetracycline hydrochloride from aqueous solution by using Fe-based metal-organic frameworks, Appl. Surf. Sci. 542 (2021) 148662. doi:10.1016/j.apsusc.2020.148662.

[4] F.E. Ahmed, R. Hashaikeh, N. Hilal, Hybrid technologies: The future of energy efficient desalination – A review, Desalination. 495 (2020) 114659. doi:10.1016/j.desal.2020.114659.

[5] A. Zaher, M. Taha, A.A. Farghali, R.K. Mahmoud, Zn/Fe LDH as a clay-like adsorbent for the removal of oxytetracycline from water: combining experimental results and molecular simulations to understand the removal mechanism, Environ. Sci. Pollut. Res. 27 (2020) 12256–12269. doi:10.1007/s11356-020-07750-3.

[6] N. Rosman, W.N.W. Salleh, M.A. Mohamed, J. Jaafar, A.F. Ismail, Z. Harun, Hybrid membrane filtration-advanced oxidation processes for removal of pharmaceutical residue, J. Colloid Interface Sci. 532 (2018) 236–260.

[7] G. Zhang, J. Ruan, T. Du, Recent advances on photocatalytic and electrochemical oxidation for ammonia treatment from water/wastewater, Acs Es&T Eng. 1 (2020) 310–325.

[8] A. Urtiaga, Electrochemical technologies combined with membrane filtration, Curr. Opin. Electrochem. 27 (2021) 100691.

[9] W.S. Koe, J.W. Lee, W.C. Chong, Y.L. Pang, L.C. Sim, An overview of photocatalytic degradation: photocatalysts, mechanisms, and development of photocatalytic membrane, Environ. Sci. Pollut. Res. 27 (2020) 2522–2565.

[10] R. Zhao, T. Ma, S. Zhao, H. Rong, Y. Tian, G. Zhu, Uniform and stable immobilization of metal-organic frameworks into chitosan matrix for enhanced tetracycline removal from water, Chem. Eng. J. 382 (2020) 122893. doi:10.1016/j.cej.2019.122893.

[11] W.S. Chai, J.Y. Cheun, P.S. Kumar, M. Mubashir, Z. Majeed, F. Banat, S.-H. Ho, P.L. Show, A review on conventional and novel materials towards heavy metal adsorption in wastewater treatment application, J. Clean. Prod. 296 (2021) 126589.

[12] J. Joseph, S. Iftekhar, V. Srivastava, Z. Fallah, E.N. Zare, M. Sillanpää, Iron-based metal-organic framework: Synthesis, structure and current technologies for water reclamation with deep insight into framework integrity, Chemosphere. 284 (2021) 131171. doi:10.1016/j.chemosphere.2021.131171.

[13] X. Zhao, M. Zheng, X. Gao, J. Zhang, E. Wang, Z. Gao, The application of MOFs-based materials for antibacterials adsorption, Coord. Chem. Rev. 440 (2021) 213970. doi:10.1016/j.ccr.2021.213970.
[14] Y. Qian, F. Zhang, H. Pang, A review of MOFs and their composites based photocatalysts: synthesis and applications, Adv. Funct. Mater. 31 (2021) 2104231.
[15] C. Du, Y. Zhang, Z. Zhang, L. Zhou, G. Yu, X. Wen, T. Chi, G. Wang, Y. Su, F. Deng, Fe-based metal organic frameworks (Fe-MOFs) for organic pollutants removal via photo-Fenton: A review, Chem. Eng. J. 431 (2022) 133932.
[16] S. Li, S. Shan, S. Chen, H. Li, Z. Li, Y. Liang, J. Fei, L. Xie, J. Li, Photocatalytic degradation of hazardous organic pollutants in water by Fe-MOFs and their composites: A review, J. Environ. Chem. Eng. 9 (2021) 105967.
[17] Y. Yang, Z. Zheng, W. Ji, J. Xu, X. Zhang, Insights to perfluorooctanoic acid adsorption micro-mechanism over Fe-based metal organic frameworks: Combining computational calculation with response surface methodology, J. Hazard. Mater. 395 (2020) 122686.
[18] X. Hu, X. Lou, C. Li, Y. Ning, Y. Liao, Q. Chen, E.S. Mananga, M. Shen, B. Hu, Facile synthesis of the Basolite F300-like nanoscale Fe-BTC framework and its lithium storage properties, RSC Adv. 6 (2016) 114483–114490.
[19] A.R. Oveisi, A. Khorramabadi-Zad, S. Daliran, Iron-based metal-organic framework, Fe(BTC): An effective dual-functional catalyst for oxidative cyclization of bisnaphthols and tandem synthesis of quinazolin-4(3H)-ones, RSC Adv. 6 (2016) 1136–1142. doi:10.1039/c5ra19013d.
[20] Q. Han, Z. Wang, X. Chen, C. Jiao, H. Li, R. Yu, Facile synthesis of Fe-based MOFs (Fe-BTC) as efficient adsorbent for water purifications, Chem. Res. Chinese Univ. 35 (2019) 564–569.
[21] N. Li, L. Zhou, X. Jin, G. Owens, Z. Chen, Simultaneous removal of tetracycline and oxytetracycline antibiotics from wastewater using a ZIF-8 metal organic-framework, J. Hazard. Mater. 366 (2019) 563–572. doi:10.1016/j.jhazmat.2018.12.047.
[22] A. Zaher, M. Taha, R.K. Mahmoud, Possible adsorption mechanisms of the removal of tetracycline from water by La-doped Zn-Fe-layered double hydroxide, J. Mol. Liq. 322 (2021) 114546. doi:10.1016/j.molliq.2020.114546.
[23] and C.M. Zhang, Tian, Li Zhang, Degradation of Ceftriaxone Sodium in Pharmaceutical Wastewater by Photocatalytic Oxidation, in: 2nd World Congr. Chem. Biotechnol. Med. (WCCBM 2020), Francis Academic Press, UK, 2020. doi:10.25236/wccbm.2020.046.
[24] M.T. da Trindade, H.R.N. Salgado, A Critical Review of Analytical Methods for Determination of Ceftriaxone Sodium, Crit. Rev. Anal. Chem. 48 (2018) 95–101. doi:10.1080/10408347.2017.1398063.
[25] M. Sanchez-Sanchez, I. de Asua, D. Ruano, K. Diaz, Direct Synthesis, Structural Features, and Enhanced Catalytic Activity of the Basolite F300-like Semiamorphous Fe-BTC Framework, Cryst. Growth Des. 15 (2015) 4498–4506. doi:10.1021/acs.cgd.5b00755.
[26] Y. Zhou, F. Fang, Q. Lv, Y. Zhang, X. Li, J. Li, Simultaneous removal of tetracycline and norfloxacin from water by iron-trimesic metal-organic frameworks, J. Environ. Chem. Eng. 10 (2022) 107403. doi:10.1016/j.jece.2022.107403.
[27] E.A. Mansour, M. Taha, R.K. Mahmoud, N. Shehata, R.M. Abdelhameed, Remarkable adsorption of oxygenated compounds from liquid fuel using copper based framework incorporated onto kaolin: Experimental and theoretical studies, Appl. Clay Sci. 216 (2022) 106371.
[28] S.M. Mahgoub, M.R. Shehata, A. Zaher, F.I.A. El-Ela, A. Farghali, R.M. Amin, R. Mahmoud, Cellulose-based activated carbon/layered double hydroxide for efficient removal of Clarithromycin residues and efficient role in the treatment of stomach ulcers and acidity problems, Int. J. Biol. Macromol. (2022).
[29] A. Zaher, M. Taha, R.K. Mahmoud, Possible adsorption mechanisms of the removal of tetracycline from water by La-doped Zn-Fe-layered double hydroxide, J. Mol. Liq. 322 (2021) 114546. doi:10.1016/j.molliq.2020.114546.
[30] M. Ghaedi, E. Shojaeipour, A.M. Ghaedi, R. Sahraei, Isotherm and kinetics study of malachite green adsorption onto copper nanowires loaded on activated carbon: artificial neural network modeling and genetic algorithm optimization, Spectrochim. Acta Part A Mol. Biomol. Spectrosc. 142 (2015) 135–149.
[31] P. Ehiomogue, I.I. Ahuchaogu, I.E. AHANEKU, REVIEW OF ADSORPTION ISOTHERMS MODELS., Acta Tech. Corviniensis-Bulletin Eng. 14 (2021).
[32] A.D. N'diaye, M.S. Kankou, Sorption of caffeine onto low cost sorbent: Application of two and three-parameter isotherm models, Appl. J. Environ. Eng. Sci. 5 (2019) 3–5.
[33] A. Kara, M. Kiliç, N. Tekin, N. Dinibütün, A. Şafakli, Application of Sepiolite-Poly(vinylimidazole) composite for the removal of Cu(II): Thermodynamics and isotherm studies, Int. J. Chem. Technol. 2 (2018) 20–33.
[34] H.A. Younes, M. Taha, R. Mahmoud, H.M. Mahmoud, R.M. Abdelhameed, High adsorption of sodium diclofenac on post-synthetic modified zirconium-based metal-organic frameworks: Experimental and theoretical studies, J. Colloid Interface Sci. 607 (2022) 334–346. doi:10.1016/j.jcis.2021.08.158.
[35] D. Supriyadi, Darmansyah, A.C. Farhani, A. Sanjaya, F. Soraya, Evaluation of kinetics adsorption models from Lampung ethnic textile industry wastewater for removal chromium onto modified activated sludge and zeolite adsorbent, IOP Conf. Ser. Earth Environ. Sci. 258 (2019) 012025. doi:10.1088/1755-1315/258/1/012025.
[36] A.A. Castañeda-Ramírez, E. Rojas-García, R. López-Medina, D.C. García-Martínez, J.

Nicolás- Antúnez, A.M. Maubert-Franco, Magnetite nanoparticles into Fe-BTC MOF as adsorbent material for the remediation of metal (Cu(II), Pb(II, As(III) and Hg(II)) ions-contaminated water, Catal. Today. (2021). doi:10.1016/j.cattod.2021.11.007.

[37] S. Shahid, K. Nijmeijer, High pressure gas separation performance of mixed-matrix polymer membranes containing mesoporous Fe(BTC), J. Memb. Sci. 459 (2014) 33–44. doi:10.1016/j.memsci.2014.02.009.

[38] D. Tocco, C. Carucci, D. Todde, K. Shortall, F. Otero, E. Sanjust, E. Magner, A. Salis, Enzyme immobilization on metal organic frameworks: Laccase from Aspergillus sp. is better adapted to ZIF-zni rather than Fe-BTC, Colloids Surfaces B Biointerfaces. 208 (2021) 112147. doi:10.1016/j.colsurfb.2021.112147.

[39] G.R. Delpiano, D. Tocco, L. Medda, E. Magner, A. Salis, Adsorption of Malachite Green and Alizarin Red S Dyes Using Fe-BTC Metal Organic Framework as Adsorbent, Int. J. Mol. Sci. 22 (2021) 788. doi:10.3390/ijms22020788.

[40] F. Dorosti, A. Alizadehdakhel, Fabrication and investigation of PEBAX/Fe-BTC, a high permeable and CO2 selective mixed matrix membrane, Chem. Eng. Res. Des. 136 (2018) 119–128. doi:10.1016/j.cherd.2018.01.029.

[41] Y. Yang, Y. Bai, F. Zhao, E. Yao, J. Yi, C. Xuan, S. Chen, Effects of metal organic framework Fe-BTC on the thermal decomposition of ammonium perchlorate, RSC Adv. 6 (2016) 67308–67314. doi:10.1039/C6RA12634K.

[42] M. Hossein Zadeh, N. Keramati, M. Mehdipour Ghazi, The effect of solvents on photocatalytic activity of Fe-BTC metal organic framework obtained via sonochemical method, Inorg. Nano-Metal Chem. 49 (2019) 448–454. doi:10.1080/24701556.2019.1661455.

[43] A. Yuan, Y. Lu, X. Zhang, Q. Chen, Y. Huang, Two-dimensional iron MOF nanosheet as a highly efficient nanozyme for glucose biosensing, J. Mater. Chem. B. 8 (2020) 9295–9303. doi:10.1039/D0TB01598A.

[44] H. Sayed, R. Mahmoud, H.F.M. Mohamed, Y. Gaber, N. Shehata, Co and Ni Double Substituted Zn-Fe Layered Double Hydroxide as 2D Nano-Adsorbent for Wastewater Treatment, Key Eng. Mater. 922 (2022) 193–213. doi:10.4028/p-tpns6c.

[45] M. Harja, G. Ciobanu, Studies on adsorption of oxytetracycline from aqueous solutions onto hydroxyapatite, Sci. Total Environ. 628 (2018) 36–43.

[46] P. Borthakur, M. Aryafard, Z. Zara, Ř. David, B. Minofar, M.R. Das, M. Vithanage, Computational and experimental assessment of pH and specific ions on the solute solvent interactions of clay-biochar composites towards tetracycline adsorption: Implications on wastewater treatment, J. Environ. Manage. 283 (2021) 111989. doi:10.1016/j.jenvman.2021.111989.

[47] M.E. Mahmoud, A.M. El-Ghanam, R.H.A. Mohamed, S.R. Saad, Enhanced adsorption of Levofloxacin and Ceftriaxone antibiotics from water by assembled composite of nanotitanium oxide/chitosan/nano-bentonite, Mater. Sci. Eng. C. 108 (2020) 110199. doi:10.1016/j.msec.2019.110199.

[48] S. bozorginia, J. Jaafari, K. Taghavi, S.D. Ashrafi, E. Roohbakhsh, D. Naghipour, Biosorption of ceftriaxone antibiotic by Pseudomonas putida from aqueous solutions, Int. J. Environ. Anal. Chem. (2021) 1–15. doi:10.1080/03067319.2021.1887858.

[49] F. Wei, Q. Ren, H. Zhang, L. Yang, H. Chen, Z. Liang, D. Chen, Removal of tetracycline hydrochloride from wastewater by Zr/Fe-MOFs/GO composites, RSC Adv. 11 (2021) 9977–9984. doi:10.1039/D1RA01027A.

[50] S.J. Olusegun, N.D.S. Mohallem, V.S.T. Ciminelli, Reducing the negative impact of ceftriaxone and doxycycline in aqueous solutions using ferrihydrite/plant-based composites: mechanism pathway, Environ. Sci. Pollut. Res. (2022). doi:10.1007/s11356-022-20561-y.

[51] M. Dávila-Estrada, J.J. Ramírez-García, M.J. Solache-Ríos, J.L. Gallegos-Pérez, Kinetic and Equilibrium Sorption Studies of Ceftriaxone and Paracetamol by Surfactant-Modified Zeolite, Water, Air, Soil Pollut. 229 (2018) 123. doi:10.1007/s11270-018-3783-4.